water

MDPI

Article

Photocatalytic Treatment of Pharmaceuticals in Real Hospital Wastewaters for Effluent Quality Amelioration

Panagiotis-Spyridon Konstas, Christina Kosma, Ioannis Konstantinou * and Triantafyllos Albanis *

Department of Chemistry, University of Ioannina, 45110 Ioannina, Greece; pkonstas@cc.uoi.gr (P.-S.K.); xkosma@gmail.com (C.K.)

* Correspondence: iokonst@uoi.gr (I.K.); talbanis@uoi.gr (T.A.); Tel.: +30-26510-08349 (I.K.); +30-26510-08348 (T.A.)

Received: 26 July 2019; Accepted: 15 October 2019; Published: 17 October 2019

Abstract: The presence of pharmaceutically active compounds (PhACs) in the wastewater effluents has confirmed that conventional wastewater treatment technologies are not sufficiently effective in the pharmaceuticals' removal. The objective of the present study was to evaluate and compare the photocatalytic degradation of PhACs using TiO_2-P25, graphitic carbon nitride (g-C_3N_4, CN) and a heterojunction of perovskite strodium titanate and graphitic carbon nitride $SrTiO_3$/g-C_3N_4 (20% g-C_3N_4, 20CNSTO) photocatalytic materials, in hospital wastewater effluents, by simulated solar irradiation. The experiments were performed by using real wastewater samples collected from the university hospital wastewater treatment plant (WWTP) effluent of Ioannina city (Northwestern Greece) and inherent pharmaceutical concentration levels. The analysis of the samples was accomplished by solid phase extraction followed by liquid chromatography-Orbitrap high-resolution mass spectrometry. In the cases of TiO_2 and CN, more than 70% of the initial concentration (e.g., venlafaxine) was degraded after 90 min, while 20CNSTO presented lower photocatalytic performance. Furthermore, some compounds were sporadically detected (e.g., fluoxetine) or their concentrations remained stable during the photocatalytic treatment time period (e.g., trimethoprim). In total 11 transformation products (TPs) were formed along the degradation processes and were identified by using liquid chromatography high resolution mass spectrometry.

Keywords: hospital wastewater; pharmaceutical compounds; photocatalysis; TiO_2; g-C_3N_4; $SrTiO_3$/g-C_3N_4; transformation products; metabolites

1. Introduction

Hospital wastewaters (HWW) are known as one of the main sources of pharmaceutical active compounds (PhACs) in the environment [1,2]. In fact, HWW is a complex water matrix, burdened with high concentrations of pharmaceuticals and metabolites, disinfectants, heavy metals, reagents, microorganisms, etc. [2,3]. Some countries consider hospital effluent as industrial wastewater and because of its characteristics, it undergoes pre-treatment before being discharged into the urban sewage system [4]. However, conventional wastewater treatment plants (WWTPs) are not manufactured to treat water containing pharmaceuticals at trace levels and consequently, the applied treatments have been found to be ineffective to remove them [1,5].

Although pharmaceuticals in hospital effluents exist in low concentrations (may vary from ng L^{-1} to mg L^{-1}), they might pose a potential threat to the ecology of the receiving environment, such as feminization of organisms, microbiological resistance or the accumulation of these compounds in

soil, plants and animals [3,6,7]. The presence of pharmaceuticals in the environment does not need to be persistent in order to cause negative effects, since the high degree of transformation or removal that they are able to incur can be overlapped by their continuous release into the environment [4]. Therefore, it is of crucial importance to treat the hospital effluents in order to avoid problems, such as the contamination and inhibition of biomass growth in conventional WWTPs [8].

Simple advanced technologies have been used in order to treat wastewater effluents, such as membrane filtration or activated carbon adsorption [5,7]. Nevertheless, such technologies do not destroy micropollutants. Therefore, advanced oxidation processes (AOPs) have been suggested as tertiary treatments in effluent wastewaters due to their versatility and ability to minimize undesirable effects into the environment [7]. In AOPs, highly reactive chemical species are formed, mostly hydroxyl radicals ($^{\bullet}$OH), which are able to degrade organic molecules into biodegradable compounds and finally, mineralize them into carbon dioxide and inorganic ions [9]. Heterogeneous semiconductor photocatalysis (PC) has become a widespread AOP method for the remediation of contamination due to its high efficiency, low price, non-toxic properties and photostability of the catalysts used [5]. AOPs have often been combined with solar irradiation since their main drawback is their high operating costs which are needed to meet the high electricity demand of the UV lamps [7,10]. Furthermore, the possible formation of oxidation intermediates which might be more toxic than the parent compound is another important drawback of AOPs, since this highlights the necessity of process optimization and performing toxicity analyses during their application [7].

Except for the most commonly used photocatalyst TiO_2-P25, other semiconductors, such as graphitic carbon nitride (g-C_3N_4) or titanate perovskites $ATiO_3$ (A = Ca, Sr, Ba, etc.), have been proven to induce the efficient elimination of organic pollutants [11–18]. TiO_2-P25 is a photocatalyst that has been widely used in many photocatalytic applications [19–29]. Furthermore, several studies have been published concerning the photocatalytic treatment of wastewaters with the use of g-C_3N_4 [30,31]. Fe-doped g-C_3N_4 and P-doped g-C_3N_4 for wastewater treatment have been synthesized [32,33]. In addition, various works concerning the photocatalytic treatment of real effluents with the use of TiO_2, g-C_3N_4, Ag/g-C_3N_4, TiO_2/Ag and g-C_3N_4/TiO_2/Fe_3O_4@SiO_2 have been conducted in recent years [34–37]. For instance, studies using heterojunctions of g-C_3N_4 like TiO_2/g-C_3N_4 for Cr(VI) removal [38] and Ag/Ag_3VO_4/g-C_3N_4 for the degradation of tetracycline in wastewaters have been published [39]. However, most studies deal with unreal high concentrations of pharmaceuticals resulting from spiking of wastewaters with the compound under study and the monitoring of degradation kinetics of individual compounds.

In view of the above, this study focuses on the application of photocatalysis for PhACs removal in real unspiked HWW effluents by combining simulated solar light and different photocatalytic semiconductors. To the best of the authors knowledge, a few studies dealing with the removal of inherent micropollutant concentration levels in effluent wastewaters by AOPs have been published [3,5,40]. Thus, the aims of the present work are: (i) To identify the PhACs present in real HWW effluents by solid phase extraction tandem liquid chromatography coupled to high-resolution mass spectrometry (SPE/LC-HRMS) analytical methodology; (ii) to evaluate and compare the photocatalytic degradation of PhACs under different semiconductors; TiO_2-P25, graphitic carbon nitride (g-C_3N_4, CN) and a heterojunction of perovskite and graphitic carbon nitride, $SrTiO_3$/g-C_3N_4 (20% g-C_3N_4, 20CNSTO) in HWW effluents using simulated solar irradiation; (iii) to identify the transformation products (TPs) formed in the different photocatalytic processes by means of LC-HRMS.

2. Materials and Methods

2.1. Reagents and Chemicals

The reference standards of pharmaceuticals were of high purity grade (>98%). Venlafaxine hydrochloride, fluoxetine hydrochloride, paroxetine, amisulpride and amitriptyline were purchased from TCI (Zwijndrecht, Belgium). Bupropion hydrochloride and mirtazapine were obtained from LGC

(Wesel, Germany). O-desmethyl venlafaxine, sertraline hydrochloride, fluvoxamine, carbamazepine, fenofibrate, citalopram, haloperidol, clozapine, trimethoprim, sulfamethoxazole, salicylic acid and diclofenac, were purchased from Sigma-Aldrich (Darmstadt, Germany). Methanol LC-MS and LC-MS grade water were purchased from Fisher Scientific (Leicestershire, UK). Formic acid (purity, 98–100%) was received from Merck KGaA (Darmstadt, Germany) and Na_2EDTA was purchased from Fisher Scientific (Leicestershire, UK). Oasis HLB (200 mg, 6 cm^3) cartridges used for solid phase extraction were purchased from Waters Corporation (Milford, MA, USA).

2.2. Hospital Wastewater Sampling

The secondary wastewater effluent samples were taken from the university hospital WWTP of Ioannina city (Epirus region, Greece). The hospital has a capacity of 800 beds and it is an academic medical center which interrelates with Ioannina's University's School of Medicine and School of Nursing. Almost 45,000 people are treated in the hospitals' care clinics while almost 130,000 people use the hospitals' casualty department every year. The HWWTP consists of a pretreatment step (grit-removal), flow equilibration tank, and a biological secondary treatment, with the final step being the disinfection with the addition of NaClO (15% solution). The hydraulic retention time (HRT) of the WWTP is 6 h, while the solid retention time (SRT) is 1.5 day. This plant discharges its effluent wastewater into the urban network which results into the municipal WWTP, therefore the assessment of its efficiency has substantial interest [41]. The samples were collected in three sampling periods, in February, March and May 2019. Amber glass bottles were used for the collection of the samples and the bottles were immediately transported to the laboratory. The samples were filtered (0.45 μm) and preserved at 4 °C until the treatments' application within 24 h.

2.3. Photocatalytic Materials

Three different semiconductor materials were used. The first includes the aeroxide TiO_2-P25 supplied from the Evonik-Degussa Corporation (BET specific surface area (SSA) 50 ± 15 m^2g^{-1}, 80% anatase, 20% rutile, average primary particle size 21 nm). The other two catalysts were the graphitic carbon nitride (g-C_3N_4, CN) (BET SSA 35 m^2g^{-1}, particle size of 25 nm, Eg = 2.82 eV) and the heterojunction g-C_3N_4/$SrTiO_3$ with g-C_3N_4 to $SrTiO_3$ ratio of 20% (20CNSTO) (BET SSA 32 m^2g^{-1}, particle size 27.6 nm, Eg values 2.80 and 3.28 in respect to g-C_3N_4 and $SrTiO_3$, respectively). The synthesis and characterization of these two materials is described elsewhere [42].

2.4. Photocatalytic Degradation Experiments

All photocatalytic degradation experiments were conducted with a Suntest XLS+ instrument (Atlas, Linsengericht, Germany) under UV-Vis irradiation (simulated solar light, $\lambda > 290$ nm). The instrument was equipped with a xenon lamp (2.2 kW), jacked with a special 290 nm cut-off glass filter and the irradiation intensity maintained at 500 Wm^{-2}. In the wastewater photocatalytic treatment process, the photocatalysts (100 mgL^{-1}) were suspended in an appropriate Pyrex glass reactor (250 mL) and magnetically stirred for 30 min in the dark in order to achieve adsorption/desorption equilibrium and along the irradiation period. During the photocatalytic process, the temperature was kept at 23 °C by water circulation in the jacket of the reactor and air-circulation. In all photocatalytic experiments, the wastewater samples were irradiated for 180 min. Periodically, the samples were withdrawn and centrifuged (Thermo Scientific, HERAUS Megafuge 8, Shanghai, China; 4400 rpm) for 20 min for the separation of the catalyst particles. Then, the centrifuged wastewater samples were filtered by 0.45 μm filters.

Two groups of experiments were conducted. The first includes photocatalytic experiments by using TiO_2 as semiconductor in HWW effluent samples of February, March and May, while the second includes photocatalytic experiments by using TiO_2, CN and 20CNSTO as semiconductors in HWW effluent samples of May.

2.5. Analytical Procedures

2.5.1. Physicochemical Properties Analysis

The chemical oxygen demand (COD), nitrate concentration (NO_3^-) and phosphate concentration (PO_4^{3-}) in the effluent were determined by means of a WTW Thermoreactor 3200 and a WTW pHotoFlex portable photometer, by following the corresponding set test for each application (WTW, Weilheim, Germany). The pH was directly measured using a Consort C932 analyzer (Constort NT, Turnhout, Belgium) with a HI-1230 pH electrode (Hanna Instruments, Woonsocket, RI, USA). Five-day biochemical oxygen demand (BOD_5) was determined by means of a WTW OxiTop OC 110 system and a WTW TS 606-G/2-i thermostat cabinet (WTW, Weilheim, Germany). Turbidity was measured by means of a Lovibond, Pc Checkit, turbidity meter (Lovibond, Dortmund, Germany). The temperature, salinity, conductivity and total dissolved solids (TDS) were determined by a WTW LF 3215 conductivity meter with TetraCon 325 Probe (WTW, Weilheim, Germany). The physicochemical properties of the collected samples are given in Table 1.

Table 1. Water quality data of the university hospital wastewater effluent of Ioannina city.

Parameter	February	March	May
Conductivity (μS/cm)	289	373	344
TDS (mg/L)	417	398	357
Temperature °C	12.2	20.8	21.9
Turbidity NTU	9.4	11.5	6.8
pH	6.8	6.5	6.7
COD (mg/L)	15	16	13
BOD_5 (mg/L)	9.6	9.6	7.9
PO_4^{3-} (mg/L)	10.7	10.7	5.06
NO_3^- (mg/L)	134.1	120.3	80.4

2.5.2. SPE Extraction and UHPLC–LTQ/Orbitrap MS Analysis

The analysis of the WWTP effluent samples and the degradation experiments were conducted with a SPE-UHPLC–LTQ/Orbitrap HRMS method. The Oasis HLB (200 mg, 6 cm^3) cartridges were selected for the determination of the target analytes. Before the extraction, an appropriate volume of 5% Na_2EDTA solution was added, in order to achieve a final concentration of 0.1% in the sample. The addition of EDTA in water before analysis has been proven with complex metals or residual metal ions, that are soluble in water, and have a high tendency to complex with the antibiotics, resulting in lower extraction efficiencies [43,44]. The preconditioning of the cartridges was performed with 5 mL of methanol and 5 mL of LC-MS grade water and then the samples (50 mL effluent at pH ≈ 7) were loaded into the cartridges and percolated with a flow rate of 10 mL/min. After the extraction, the cartridges were washed with 5 mL of LC-MS grade water and dried for 15 min under vacuum. Following this, the elution of the analytes was performed twice with 5 mL of LC-MS grade methanol at 1 mL/min and the combined extracts were evaporated to dryness under a gentle stream of nitrogen at 40 °C by means of Techne Dri-Block heater Model DB-3D. Finally, reconstitution was done with 250 μL of methanol: water 20:80 (*v/v*) with 0.1% formic acid and the samples were stored at −20 °C until analysis.

Analysis of the samples was perfomed by a UHPLC Accela LC system, connected with a hybrid LTQ-FT Orbitrap XL 2.5.5 SP1 mass spectrometer which was equipped with electrospray ionization source (ESI) (Thermo Fisher Scientific, Inc., GmbH, Bremen, Germany). The full scan in positive (PI) and negative (NI) ionization mode was acquired, for identification and quantification purposes. The data-dependent acquisition (full MS/dd-MS^2) based on collision induced dissociation (CID) was performed and the mass tolerance window was set to 5 ppm. Thermo Xcalibur 2.1 software (Thermo Electron, San Jose, CA, USA) was used for the processing of the data. A reversed phase SpeedCore C18 analytical column with 50 mm × 2.1 mm, 2.6 μm particle size (Fortis Technologies, Cheshire, UK) was used for the chromatographic separation. In PI, the samples were separated at 27 °C, with 0.1% formic

acid in LC-MS grade water (mobile phase A) and 0.1% formic acid in LC-MS grade methanol (mobile phase B). The elution gradient in PI started with 95% A (initial conditions), kept at 95% for 1 min, progressed to 30% in 3 min, then progressed to 0% in 6 min, and returned to the initial conditions after 3 with 1 min re-equilibration of the column. The total run time was 10 min. In NI, the samples were separated at 27 °C, with LC-MS grade water (mobile phase A) and LC-MS grade methanol (mobile phase B). The elution gradient in NI started with 90% A (initial conditions), kept at 90% for 0.5 min, progressed to 30% in 2 min, reaching 10% in 3 min, decreased in 5% at 3.9 min, decreased in 0% at 4.5 min, remained 0% for 0.5 min, and returned to the initial conditions after 1 min with 2 min re-equilibration of the column. The total run time was 8 min. The flow rate in PI and NI was 0.4 mL/min with an injection volume of 5 and 20 μL, respectively.

Concerning validation of the method, the limits of detection (LODs) and quantification (LOQs) of the target compounds were determined as the minimum detectable amount of the analyte, which provided signal to noise ratio 3:1 and 10:1, respectively. The LODs ranged between 0.5 and 9.0 ng/L while the LOQs ranged between 1.1 and 26.7 ng/L, for carbamazepine and salicylic acid, respectively. In order to identify the presence of possible transformation products (TPS), concerning the PhACs which presented degradation profile, an in-house database was created, containing theoretical exact masses of metabolite/TPs determined in previous works [22,45–52]. The target compounds included in the database were detected in the samples based on criteria such as the retention time, mass error of the suspected analyte within ±5 ppm, isotopic profile matching for each molecular formula and MS^2 fragmentation pattern [6].

3. Results and Discussion

3.1. Degradation of Pharmaceuticals in the Hospital WWTP Effluent

The Orbitrap HRMS analysis revealed the presence of 19 target pharmaceuticals in the hospital effluent belonging to various therapeutic categories, which were identified and quantified in all cases. The concentrations of the above compounds in the effluents are given in Table 2. The residual concentration of pharmaceuticals in the secondary effluent depends on the biodegradability of the chemicals and treatment capacity of the secondary biological treatment processes. In particular, depending on their input concentration level and removal efficiencies, they can be discriminated in two groups. The first group includes compounds that presented frequent detection in the secondary effluents and therefore their photocatalytic degradation kinetic was systematically assessed. These compounds were the antidepressant venlafaxine (VNX) and its metabolite O-desmethyl venlafaxine (ODV), the antipsychotic amisulpride (AMS), the antibiotic sulfamethoxazole (SMX) and the antiepileptic carbamazepine (CBZ). Their degradation followed pseudo-first order kinetics. The rate constant k was calculated from the equation:

$$C_t = C_0\, e^{-kt} \quad (1)$$

where C_t is the concentration at time t and C_0 the initial concentration. At the time, that concentration reduces to 50% of its initial amount and the half-life is calculated by t1/2 = ln2/k [53–55]. Table 3 shows the photocatalytic degradation rate constants of the above compounds, half-lives and correlation coefficients, while Figure 1 presents their degradation rate constants in relation with COD, TDS and conductivity in aqueous TiO_2 suspensions in the three sampling months.

All compounds presented higher degradation rates in May (k ranged between 0.0128 min^{-1} for SMX and 0.0177 min^{-1} for ODV) and lower in March (k = 0.0022 min^{-1} for SMX). Only AMS degraded at a lower rate in February (k = 0.0046 min^{-1}). Furthermore, in May, after 120 min, an average degradation of more than 80% was observed for VNX, ODV, AMS, SMX and CBZ. In March, more than 65% of VNX, ODV and AMS were degraded after 120 min, while SMX and CBZ were degraded at much smaller rates. Similar results were shown in February where VNX and ODV presented degradation > 75% after 120 min, while AMS and CBZ presented 42% and 57% elimination, respectively.

Table 2. Concentration levels (ng/L) of pharmaceutically active compounds (PhACs) identified in real hospital wastewater treatment plants (WWTP) effluent in the three sampling campaigns by UHPLC–LTQ/Orbitrap MS.

Pharmaceuticals	Ionization	Concentration (ng/L)		
	Mode	February	March	May
Analgesic/Anti-inflammatory				
Salicylic acid	−	236.4	239.9	<LOQ
Diclofenac	−	181.1	181.0	79.2
Lipid regulator				
Fenofibrate	+	n.d.	n.d.	128.9
Antibiotic				
Trimethoprim	+	n.d.	97.0	21.5
Sulfamethoxazole	+	n.d.	157.9	349.8
Antidepressant				
Venlafaxine	+	434.2	412.5	391.2
O-desmethyl venlafaxine	+	691.4	1871.0	748.5
Mirtazapine	+	n.d.	n.d.	43.2
Bupropion	+	n.d.	n.d.	15.8
Paroxetine	+	32.4	n.d.	n.d.
Fluoxetine	+	n.d.	36.7	n.d.
Sertraline	+	n.d.	68.4	n.d.
Citalopram	+	102.4	55.9	39.4
Amitryptiline	+	23.0	n.d.	n.d.
Fluvoxamine	+	n.d.	n.d.	8.5
Antiepiliptic				
Carbamazepine	+	388.2	266.7	242.0
Antipsychotic				
Haloperidol	+	42.0	n.d.	n.d.
Clozapine	+	67.8	n.d.	n.d.
Amisulpride	+	102.0	929.4	505.5

Table 3. Kinetic parameters of PhACs photocatalytic degradation in TiO_2 suspensions in the three sampling months in hospital wastewater effluent.

Compound	February			March			May		
	k (min^{-1})	$t_{1/2}$ (min)	R^2	k (min^{-1})	$t_{1/2}$ (min)	R^2	k (min^{-1})	$t_{1/2}$ (min)	R^2
VNX	0.0124	55.90	0.9971	0.0104	66.50	0.9918	0.0176	39.38	0.9956
ODV	0.0131	52.91	0.9971	0.0097	71.46	0.9902	0.0177	39.16	0.9900
AMS	0.0046	150.68	0.9922	0.0108	64.80	0.9915	0.0155	44.52	0.9900
SMX	-	-	-	0.0022	315.07	0.9914	0.0128	54.15	0.9937
CBZ	0.0071	97.63	0.9908	0.0054	128.36	0.9933	0.0161	43.05	0.9962

The second group consists of sporadically detected compounds in the effluents, which can further be sub-classed into: (a) Those compounds which their degradation was accomplished within 45 min (e.g., haloperidole, paroxetine, clozapine, amitriptyline, sertraline, diclofenac, fluoxetine and mirtazapine) and (b) those compounds whose initial concentration (traces in most cases) remained nearly stable during the photocatalytic process (e.g., trimethoprim, citalopram, fluvoxamine, bupropion, fenofibrate and salicylic acid). According to Czech et al. [56], high initial concentrations of PhACs might favor their removal as their initial photocatalytic oxidation rate is increased. The same authors reported also that a higher wavelength of irradiation and lower concentrations of micropollutants are not beneficial in wastewater photocatalytic treatment. Furthermore, the presence of other molecules in the effluents may hinder the total photocatalytic degradation of micropollutants which are present

in trace levels, since this treatment includes various reactions occurring on and close to the catalysts surface [56]. For instance, Choin et al. [57] reported the possibility that inorganic ions present in the effluents (such as NH_4^+, NO_3^- and HCO_3^-) alter the surface charge of TiO_2 and hence, its adsorption preference towards micropollutants. In addition, the effluent organic interferences, such as humic components, might hinder the photocatalytic efficiency of micropollutants: (i) By disposing a significant amount of organic moieties to scavenge photogenerated •OH and (ii) by absorbing onto TiO_2, thereby reducing the available active sites of the surface, and inducing oxidation with surface-bound·•OH [57].

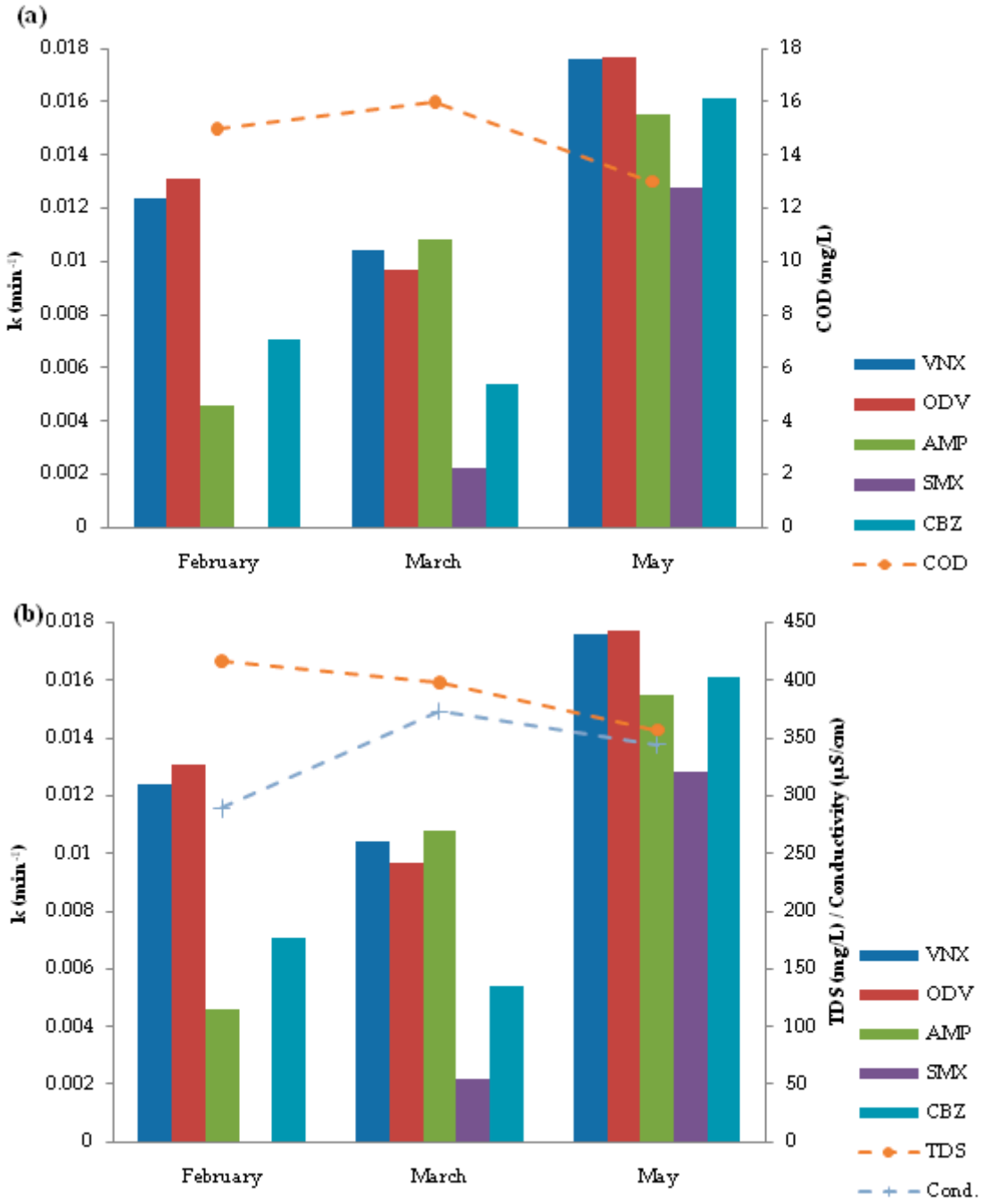

Figure 1. Degradation rate constants of pharmaceutically active compounds (PhACs) in relation with (**a**) chemical oxygen demand (COD) and (**b**) total dissolved solids (TDS) and conductivity, in TiO_2 suspensions in the three sampling months.

In this context, in Figure 1, it is shown that higher degradation rates are accomplished for lower initial concentrations of COD (Figure 1a) and TDS (Figure 1b). Similar results were reported by Choin et al. [57] where pharmaceuticals' degradation using TiO_2-based catalysts decreased when the concentration of dissolved organic carbon was increased. This was attributed to the competition between the target compound and the organic matter which existed in the effluent, for the active sites of the surface and the photogenerated •OH. As for the initial conductivity of the effluent samples concerns, it was shown that it did not notably affect the degradation efficiency of the target pharmaceuticals (Figure 1b).

It is worth noticing that although salicylic (SA) acid was detected at concentrations of 236.4 ng/L in February and 239.9 ng/L in March, no degradation during the photocatalytic treatment was observed. SA is the major metabolite of acetylsalicylic acid (aspirin) which is a common non-steroidal anti-inflammatory drug. In addition, there are several other sources of SA since it is also used as an additive in some skin-care products, in toothpastes and as a food preservative [6]. In a previous study using TiO_2, the highest degradation of SA was found at high initial concentrations. In particular, its photocatalytic degradation was faster with an initial concentration of 50 mg/L than 10 mg/L [58]. Furthermore, in another work accomplished by Vilhunen et al. [59], the effect of the initial concentration of SA on its degradation rate was also studied by using TiO_2 T300 as a catalyst. Similarly, the higher degradation rates have been recorded in a higher initial concentration of SA. These results might be explained by the fact that at higher concentrations, more SA molecules are nearby or sorbed onto the catalyst's surface and ready to react with·•OH [59]. Taking the above into consideration, in the present work, SA persistence could be explained by assuming competitive adsorption of other constituents or pharmaceuticals contained in wastewaters onto the catalysts' surface as well as the higher reactivity of the other constituents towards photogenerated hydroxyl radicals and/or positive holes.

The next step was to evaluate and compare the photocatalytic degradation of PhACs under TiO_2, CN and 20CNSTO processes, in hospital wastewater effluents by simulated solar irradiation (Table 4). Preliminary experiments concerning photolysis and adsorption (in TiO_2, CN and 20CNSTO materials) were conducted. Photodegradation experiments (Figure 2) showed that VNX and SMX concentrations remained stable during the process, while for ODV, AMS and CBZ, the results showed that 8%, 11% and 12% of the initial concentration was degraded after 180 min of irradiation, indicating no significant contribution to their degradation. Furthermore, the experiments under dark conditions which were performed in order to establish the adsorption-desorption equilibrium of the target compounds showed limited adsorption of the target compounds on the catalyst's surface i.e., less than 9%, at equilibrium (30 min). These very low adsorption phenomena are due to the catalysts small specific surface areas, since they display 50, 35 and 32 m^2g^{-1} for TiO_2, CN and 20CNSTO, respectively [42].

Table 4. Kinetic parameters of PhACs photocatalytic degradation in hospital wastewater effluent using TiO_2, CN and 20CNSTO.

Compound	TiO_2			CN			20CNSTO		
	k (min^{-1})	$t_{1/2}$ (min)	R^2	k (min^{-1})	$t_{1/2}$ (min)	R^2	k (min^{-1})	$t_{1/2}$ (min)	R^2
VNX	0.0176	39.38	0.9956	0.0327	21.2	0.9909	0.0038	182.41	0.9913
ODV	0.0177	39.16	0.9900	0.0148	46.83	0.9903	0.0040	173.29	0.9902
AMS	0.0155	44.52	0.9900	0.0308	22.50	0.9970	0.0153	45.30	0.9901
SMX	0.0128	54.15	0.9937	0.0103	67.30	0.9902	-	-	-
CBZ	0.0161	43.05	0.9962	0.0232	29.88	0.9905	0.0035	198.04	0.9901

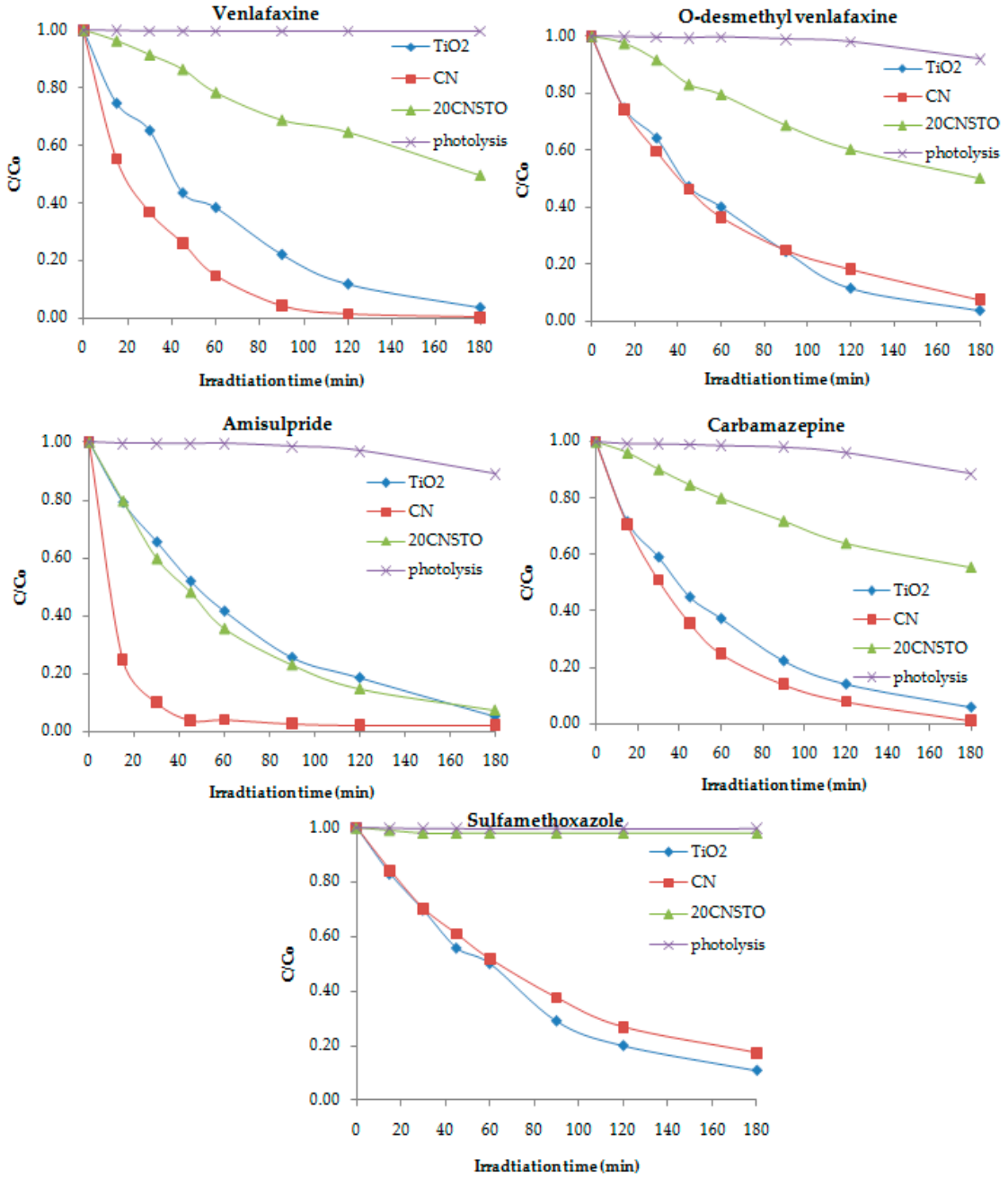

Figure 2. Photolytic and photocatalytic degradation of PhACs versus irradiation time in hospital wastewater effluent using TiO_2, CN and 20CNSTO.

In most of the cases, the photocatalytic degradation of the studied compounds presented to be higher in CN and TiO_2, while 20CNSTO presented lower photocatalytic performances (see Figure 2). In particular, concerning the antidepressant VNX, after 90 min of irradiation with CN, 96% of the initial concentration was degraded, presenting a rate constant of k = 0.0327 min^{-1} and a half-life of $t_{1/2}$ = 21.2 min. The lower degradation performances of 78% and 31% were recorded in this case for TiO_2 and 20CNSTO, respectively. The ODV degradation was slightly higher with TiO_2 (k = 0.0177 min^{-1}) than with CN (k = 0.0148 min^{-1}), presenting after a 90 min removal performance of 76% and 75%, respectively.

The photocatalytic efficiency of AMS and CBZ was significantly enhanced in the presence of CN, showing a degradation of 98% ($t_{1/2}$ = 22.5 min) and 86% ($t_{1/2}$=29.9 min), respectively after 90 min of irradiation. Their degradation constant rates followed the order: CN> TiO_2> 20CNSTO. The antibiotic

SMX, in the presence of TiO_2 and CN followed pseudo-first order kinetics, while low degradation was recorded in the presence of 20CNSTO. More specifically, after 90 min of irradiation, 71% of the initial compound was degraded with TiO_2 and 62% with CN. As for the activity of 20CNSTO concerns, the concentration of SMX remained nearly stable during the 180 min of irradiation.

In addition, the physical-chemical parameters of the hospital wastewater before and after the photocatalytic treatment with the three catalysts are given in Table 5. After photocatalysis, COD decreased moderately due to degradation of PhACs and wastewater organic compounds [10]. This moderate decrease denotes that the decomposition products of PhACs and organic matter substances still contribute in the COD pool. In addition, the evolution of inorganic ions released into the solutions after 180 min of irradiation showed an increment of nitrates (NO_3^-) in all cases following the order CN > TiO_2 > 20CNSTO. Phosphate ions (PO_4^{3-}) were found in relatively lower concentrations in the treated effluents with all catalysts indicating that they might be absorbed on the photocatalysts' surface [60]. As for conductivity concerns, its enhancement can be attributed to the increment of mineralization during the photocatalytic process.

Table 5. Physicochemical characteristics of the hospital effluent wastewater before and after the photocatalytic degradation in May.

Parameter	Hospital Wastewater before PC	Hospital Wastewater after PC-TiO_2-P25	Hospital Wastewater after PC-CN	Hospital Wastewater after PC-20CNSTO
Conductivity (μS/cm)	344	403	393	407
TDS (mg/L)	357	371	372	373
pH	6.7	6.7	7	6.8
COD (mg/L)	13	<10	<10	<10
PO_4^{3-} (mg/L)	5.06	3.38	4.22	3.8
NO_3^- (mg/L)	80.4	158.7	165.1	120.4

3.2. Transformation Products/Metabolites Identification

The identification of TPs/metabolites is of crucial importance since it provides information concerning not only the risk assessment on the drug residues in the environment, but also the design of new treatment-technologies [22]. In order to identify the possible metabolites/TPs present in the samples, each one was analyzed by the UHPLC-Orbitrap MS as previously described in Section 2.5.2. A purpose-built database for the five pharmaceuticals that presented high concentrations and frequent detection in the secondary effluents was elaborated. These were VNX, ODV, AMS, CBZ and SMX. A number of metabolites/TPs in the studied samples were identified, despite of the fact that there was no the availability of the reference standards [61]. Table 6 summarizes the relevant analytical information concerning the metabolites/TPs identified in the three studied catalysts. Most of the compounds were present in the different treatment procedures, showing that similar reaction mechanisms occurred and in all cases low mass errors were observed (<5 ppm) [4].

According to Table 6, various TPs/metabolites were identified for the studied compounds. VNX is mainly metabolized in humans in ODV. According to previous studies, N-desmethyl venlafaxine (NDV) is also produced during metabolism but to a less extent since it has been proved that O-demehtylation accounts for 90%, while N-demethylation for 10% of oxidative metabolism [22]. Both ODV and NDV have an *m/z* 264.1958 and elemental composition $C_{16}H_{26}NO_2^+$. Lambropoulou et al. [22] confirmed the identities of the two compounds and ODV was assigned as the first eluted compound while the second-one was assigned to NDV. In our study, in all cases, only ODV was identified and quantified, also due to the availability of a reference standard. Additionally, MS^2 product ion with *m/z* 246.1852 ($C_{16}H_{24}NO^+$), corresponded to H_2O loss which further supported the identification.

Table 6. Retention time (R_t), elemental formula, experimental and theoretical mass, mass error deviation and double bond and ring equivalent number (RDB) of metabolites/transformation products (TPs) identified during the three catalysts treatment by UHPLC-Orbitrap MS using the in-house database (molecular ions in bold).

TPs/ Metabolites	R_t (min)	Elemental Formula $[M + H]^+$	Accurate Mass		Error (ppm)	DBE	Catalyst Occurrence
			Theor.	Exper.			
VNX	**3.14**	**$C_{17}H_{28}NO_2$**	**278.2115**	**278.2126**	**3.934**	**4.5**	**TiO_2, CN, 20CNSTO**
VNX-TP1	3.02	$C_{16}H_{24}NO_2$	262.1802	262.1805	1.238	5.5	TiO_2, CN, 20CNSTO
VNX-TP2	2.15	$C_{16}H_{26}NO_3$	280.1903	280.1912	1.784	4.5	TiO_2, CN
VNX-TP3a	2.36	$C_{15}H_{24}NO_2$	250.1802	250.1808	2.776	4.5	TiO_2, CN, 20CNSTO
VNX-TP3b	2.88	$C_{15}H_{24}NO_2$	250.1802	250.1811	3.575	4.5	TiO_2, CN, 20CNSTO
ODV	**2.72**	**$C_{16}H_{26}NO_2$**	**264.1958**	**264.1967**	**3.575**	**4.5**	**TiO_2, CN, 20CNSTO**
ODV-TP1	2.17	$C_{16}H_{24}NO$	246.1852	246.1854	0.646	5.5	TiO_2, CN, 20CNSTO
AMS	**2.53**	**$C_{17}H_{28}N_3O_4S$**	**370.1795**	**370.1805**	**2.719**	**5.5**	**TiO_2, CN, 20CNSTO**
AMS-TP1	2.69	$C_{17}H_{28}N_3O_5S$	386.1744	386.1747	0.678	5.5	TiO_2, CN, 20CNSTO
CBZ	**3.60**	**$C_{15}H_{13}N_2O$**	**237.1022**	**237.1028**	**2.279**	**10.5**	**TiO_2, CN, 20CNSTO**
CBZ-TP1	3.20	$C_{15}H_{13}N_2O_2$	253.0972	253.0976	1.682	10.5	TiO_2, CN, 20CNSTO
CBZ-TP2	3.28	$C_{15}H_{13}N_2O_2$	253.0972	253.0976	1.682	10.5	TiO_2, CN, 20CNSTO
CBZ-TP3	3.40	$C_{15}H_{13}N_2O_2$	253.0972	253.0974	0.971	10.5	TiO_2, CN, 20CNSTO
CBZ-TP4	3.55	$C_{15}H_{13}N_2O_2$	253.0972	253.0982	4.211	10.5	TiO_2, CN
CBZ-TP5	3.22	$C_{15}H_{15}N_2O_3$	271.1077	271.1083	2.955	9.5	TiO_2, CN, 20CNSTO
SMX	**2.77**	**$C_{10}H_{12}N_3O_3S$**	**254.0594**	**254.0600**	**0.612**	**6.5**	**TiO_2, CN, 20CNSTO**

According to our results, a total of three TPs were found for VNX, which can also be designated as intermediates originating from its metabolite ODV. The first with *m/z* 262.1802 and elemental composition $C_{16}H_{24}NO_2^+$ could be generated from further oxidation of ODV with *m/z* 264.1958 and an elemental composition of, $C_{16}H_{26}NO_2^+$. The mass loss of approximately 2 Da could be explained either by the formation of a double bond or by an oxidative ring closing reaction [22]. The second TP identified with *m/z* 280.1903 and elemental composition $C_{16}H_{26}NO_3^+$ was generated from the hydroxylation of TP 264 (ODV). The MS^2 fragmentation of the above TPs with *m/z* 262.1802 and *m/z* 280.1903 exhibited ions at *m/z* 244.165 ($C_{16}H_{22}NO^+$) and *m/z* 262.1802 ($C_{16}H_{24}NO_2^+$), respectively, derived both from the loss of H_2O. Two isomers were detected for the third TP. This is a di-desmethyl VNX product with *m/z* 250.1802 and an elemental composition of $C_{15}H_{24}NO_2^+$. Garcia-Galan et al. [45] also reported the finding of these two isomers in UV/H_2O_2 oxidation of VNX and ODV. The above TPs were previously identified by Lambropoulou et al. [22] as intermediate products after photocatalytic degradation of VNX using TiO_2/UV process. Finally, the hydroxylated moiety of ODV was detected with *m/z* 278.1751 and an elemental composition of $C_{16}H_{24}NO_3^+$ [45].

Regarding AMS, only one TP was observed. This TP exhibited an *m/z* of 386.1744 corresponding to the elemental composition $C_{17}H_{28}N_3O_5S^+$ by the addition of an oxygen atom. This TP has been previously reported by Skibinski et al. [46] as a TP formed after a photodegradation study of AMS.

Concerning CBZ, the analysis allowed the identification of five metabolites under the different photocatalytic treatments. The principal metabolite of carbamazepine is carbamazepine-10,11-epoxide (CBZ-EP) which is further metabolized into 10,11-dihydro-10,11-trans-dihydroxycarbamazepine (Trans-CBZ). The keto analogue of CBZ, known as Oxcarbazepine (OxCBZ), generates common TPs with those of CBZ, such as Trans-CBZ and 10-hydroxy-10,11-dihydrocarbamazepine (licarbazepine, LIC). Various TPs of carbamazepine have been identified in surface and ground waters, such as 2-hydroxycarbamazepine (2OH-CBZ), 3-hydroxycarbamazepine (3OH-CBZ), CBZ-EP, 9,10-dihydro-9-oxoacridine (acridone) and acridine [50].

In our study, four peaks were found with the *m/z* 253.0972 corresponding to an elemental composition of $C_{15}H_{15}N_2O_2^+$. The above *m/z* accounts either for CBZ-EP or OxCBZ or 2OH-CBZ or 3OH-CBZ [50]. Since in the present study real effluent wastewater samples were studied, the

metabolites of the parent compounds existed in traces, therefore due to the lack of MS^2-MS^3 mass spectra it was not possible to clearly identify which peak corresponded to the respective metabolites. In this case, further studies by applying commercially available standards are needed. The fifth metabolite with *m/z* 271.1077 and an elemental composition of $C_{15}H_{15}N_3O_2^+$ is the Trans-CBZ-diol, generated from the addition of two hydroxyl groups in the parent CBZ [48].

As for SMX concerns, none of the TPs recorded from the literature were identified in the analyzed samples. It is possible that some other TPs could have been produced during the photocatalytic processes in all catalysts examined. However, their low formation during the process did not make it possible for their identification. Furthermore, it is worth noticing that in the studies where transformation products are suggested, usually only one drug is studied at high initial concentrations (normally in order of tens of mgL^{-1}) [4]. In contrast, in the present study, real effluent samples were studied, therefore, the identification of TPs at very low concentrations was a challenge. The metabolites/TPs evolution as a function of irradiation time was also determined by UHPLC-Orbitrap MS and their evolution profiles found under TiO_2 and CN photocatalytic treatment in May are depicted in Figure 3. All TPs were completely or nearly degraded within 180 min.

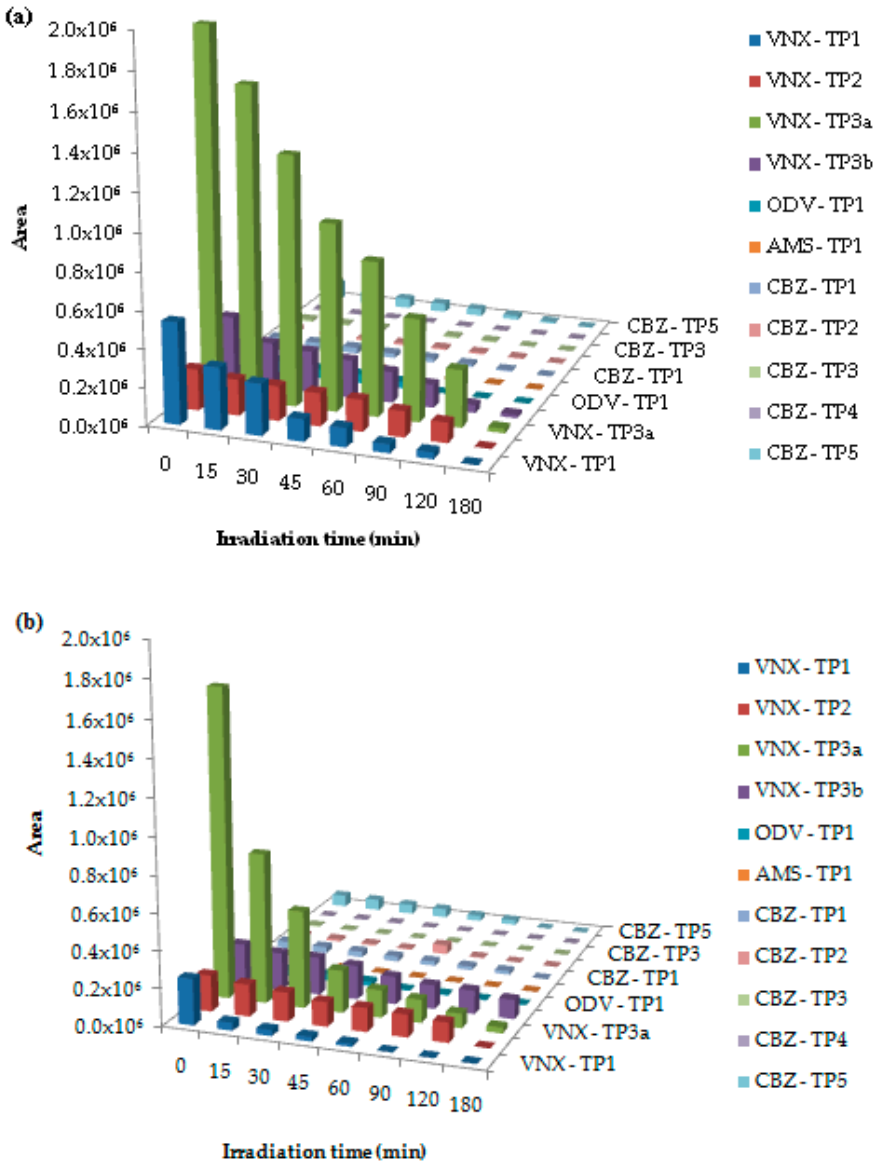

Figure 3. Evolution of identified metabolites/TPs in (**a**) TiO_2 and (**b**) CN photocatalytic treatment based on UHPLC-Orbitrap MS.

4. Conclusions

This study focused on the impact of different catalysts, TiO_2-P25, CN and 20CNSTO on the heterogeneous photocatalytic treatment of pharmaceutical micropollutants in real hospital effluent wastewater samples. An analysis of the samples was accomplished by SPE followed by UHPLC–LTQ/Orbitrap HRMS where 19 target pharmaceuticals were detected in the effluent. Depending on their initial concentrations and removal efficiencies, the above compounds were discriminated: (a) Those that presented frequent detection and their photocatalytic degradation was assessed (VNX, ODV, AMS, SMX, CBZ) and (b) to those that were sporadically detected (e.g., fluoxetine and bupropion). Therefore, it was not feasible to monitor their photocatalytic degradation since in some cases, the presence of other molecules in the effluents may hinder their total photocatalytic efficiency.

The photocatalytic pattern of the compounds belonging to the first group followed the pseudo-first order kinetics. TiO_2 and CN presented higher photocatalytic performance than 20CNSTO in all cases with CN presenting similar or better degradation rates that TiO_2, depending on the pharmaceutical compound. The physical-chemical measurements of the parameters before and after the photocatalytic treatment with the three catalysts revealed degradation-mineralization of the micropollutants present in the effluent wastewater. In order to detect the occurrence of possible metabolites/TPs formed, a purpose-built database for the five pharmaceuticals that presented high concentrations and frequent detection in the secondary effluents, was elaborated for analysis of the samples by UHPLC-Orbitrap MS. This allowed the identification of 11 TPs generated during the photocatalytic processes using accurate mass values and fragmentation patterns.

Author Contributions: Conceptualization and methodology, I.K. and T.A.; formal analysis, P.-S.K.; C.K.; I.K.; investigation, P.-S.K.; C.K. and I.K.; data curation, P.-S.K.; C.K.; writing-original draft preparation, P.-S.K.; C.K. and I.K.; writing-review and editing, P.-S.K.; C.K.; I.K. and T.A.; validation and visualization, P.-S.K. and C.K.; supervision, T.A. and I.K.

Funding: This research was co-funded by the European Union and National Funds of the participating countries (Interreg-IPA CBC, Greece-Albania, "PhaRem").

Acknowledgments: The authors would like to thank the Unit of Environmental, Organic and Biochemical high resolution analysis-ORBITRAP-LC–MS of the University of Ioannina for providing access to the facilities.

Conflicts of Interest: The authors declare no conflicts of interest.

References

1. Kosma, C.I.; Lambropoulou, D.A.; Albanis, T.A. Investigation of PPCPs in wastewater treatment plants in Greece: Occurrence, removal and environmental risk assessment. *Sci. Total Environ.* **2014**, *466–467*, 421–438. [CrossRef]
2. Serna-Galvis, E.A.; Silva-Agredo, J.; Botero-Coy, A.M.; Moncayo-Lasso, A.; Hernández, F.; Torres-Palma, R.A. Effective elimination of fifteen relevant pharmaceuticals in hospital wastewater from Colombia by combination of a biological system with a sonochemical process. *Sci. Total Environ.* **2019**, *670*, 623–632. [CrossRef] [PubMed]
3. Souza, F.S.; Da Silva, V.V.; Rosin, C.K.; Hainzenreder, L.; Arenzon, A.; Pizzolato, T.; Jank, L.; Feris, L.A. Determination of pharmaceutical compounds in hospital wastewater and their elimination by advanced oxidation processes. *J. Environ. Sci. Health. Part A* **2017**, *53*, 213–221. [CrossRef] [PubMed]
4. Cuervo Lumbaque, E.; Cardoso, R.M.; Dallegrave, A.; dos Santos, L.O.; Ibáñez, M.; Hernández, F.; Sirtori, C. Pharmaceutical removal from different water matrixes by Fenton process at near-neutral pH: Doehlert design and transformation products identification by UHPLC-QTOF MS using a purpose-built database. *J. Environ. Chem. Eng.* **2018**, *6*, 3951–3961. [CrossRef]
5. Teixeira, S.; Gurke, R.; Eckert, H.; Kuhn, K.; Fauler, J.; Cuniberti, G. Photocatalytic degradation of pharmaceuticals present in conventional treated wastewater by nanoparticle suspensions. *J. Environ. Chem. Eng.* **2016**, *4*, 287–292. [CrossRef]
6. Kosma, C.I.; Lambropoulou, D.A.; Albanis, T.A. Comprehensive study of the antidiabetic drug metformin and its transformation product guanylurea in Greek wastewaters. *Water Res.* **2015**, *70*, 436–448. [CrossRef]

7. Prieto-Rodriguez, L.; Oller, I.; Klamerth, N.; Aguera, A.; Rodrıguez, E.M.; Malato, S. Application of solar AOPs and ozonation for elimination of micropollutants in municipal wastewater treatment plant effluents. *Water Res.* **2013**, *47*, 1521–1528. [CrossRef]
8. Lima Perini, J.A.; Tonetti, A.L.; Vidal, C.; Montagner, C.C.; Pupo Nogueira, R.F. Simultaneous degradation of ciprofloxacin, amoxicillin, sulfathiazole and sulfamethazine, and disinfection of hospital effluent after biological treatment via photo-Fenton process under ultraviolet germicidal irradiation. *Appl. Catal. B Environ.* **2018**, *224*, 761–771. [CrossRef]
9. Rioja, N.; Benguria, P.; Peñas, F.J.; Zorita, S. Competitive removal of pharmaceuticals from environmental waters by adsorption and photocatalytic degradation. *Environ. Sci. Pollut. Res.* **2014**, *21*, 11168–11177. [CrossRef]
10. He, Y.; Sutton, N.B.; Rijnaarts, H.H.H.; Langenhoff, A.A.M. Degradation of pharmaceuticals in wastewater using immobilized TiO_2 photocatalysis under simulated solar irradiation. *Appl. Catal. B Environ.* **2016**, *182*, 132–141. [CrossRef]
11. Konstas, P.-S.; Konstantinou, I.; Petrakis, D.; Albanis, T. Development of $SrTiO_3$ Photocatalysts with Visible Light Response Using Amino Acids as Dopant Sources for the Degradation of Organic Pollutants in Aqueous Systems. *Catalysts* **2018**, *8*, 528. [CrossRef]
12. Li, G.; Wu, Y.; Zhang, M.; Chu, B.; Huang, W.-Y.; Fan, M.; Dong, L.; Li, B. The enhanced removal of toxic Cr(VI) in wastewater by synthetic TiO_2/g-C_3N_4 microspheres/rGO photocatalyst under irradiation of visible light. *Ind. Eng. Chem. Res.* **2019**, *58*, 8979–8989. [CrossRef]
13. Li, H.; Shan, C.; Pan, B. Development of Fe-doped g-C_3N_4/graphitemediated peroxymonosulfate activation for degradation of aromatic pollutants via nonradical pathway. *Sci. Total Environ.* **2019**, *675*, 62–72. [CrossRef] [PubMed]
14. Qu, L.-L.; Genga, Z.-Q.; Wang, W.; Yang, K.-C.; Wang, W.-P.; Han, C.-Q.; Yang, G.-H.; Vajtai, R.; Li, D.-W.; Ajayan, P.M. Recyclable three-dimensional Ag nanorod arrays decorated with O-g-C_3N_4 for highly sensitive SERS sensing of organic pollutants. *J. Hazard. Mater.* **2019**, *379*, 120823. [CrossRef]
15. Li, X.; Qian, X.; An, X.; Huang, J. Preparation of a novel composite comprising biochar skeleton and "chrysanthemum" g-C_3N_4 for enhanced visible light photocatalytic degradation of formaldehyde. *Appl. Surf. Sci.* **2019**, *487*, 1262–1270. [CrossRef]
16. Alammar, T.; Hamm, I.; Wark, M.; Mudring, A.-V. Low-temperature route to metal titanate perovskite nanoparticles for photocatalytic applications. *Appl. Catal. B Environ.* **2015**, *178*, 20–28. [CrossRef]
17. Rosy, A.; Kalpana, G. Reduced graphene oxide/strontium titanate heterostructured nanocomposite as sunlight driven photocatalyst for degradation of organic dye pollutants. *Curr. Appl. Phys.* **2018**, *18*, 1026–1033. [CrossRef]
18. Kumar, A.; Khan, M.; Zeng, X.; Lo, I.M.C. Development of g-C_3N_4/TiO_2/Fe_3O_4@SiO_2 heterojunction via sol-gel route: A magnetically recyclable direct contact Z-scheme nanophotocatalyst for enhanced photocatalytic removal of ibuprofen from real sewage effluent under visible light. *Chem. Eng. J.* **2018**, *353*, 645–656. [CrossRef]
19. Evgenidou, E.; Konstantinou, I.; Fytianos, K.; Poulios, I.; Albanis, T. Photocatalytic oxidation of methyl parathion over TiO_2 and ZnO suspensions. *Catal. Today* **2007**, *124*, 156–162. [CrossRef]
20. Lambropoulou, D.A.; Hernando, M.D.; Konstantinou, I.K.; Thurmanb, E.M.; Ferrer, I.; Albanis, T.A.; Fernandez-Alba, A.R. Identification of photocatalytic degradation products of bezafibrate in TiO2 aqueous suspensions by liquid and gas chromatography. *J. Chromatogr. A* **2008**, *1183*, 38–48. [CrossRef]
21. Lambropoulou, D.A.; Konstantinou, I.K.; Albanis, T.A.; Fernandez-Alba, A.R. Photocatalytic degradation of the fungicide Fenhexamid in aqueous TiO_2 suspensions: Identification of intermediates products and reaction pathways. *Chemosphere* **2011**, *83*, 367–378. [CrossRef] [PubMed]
22. Lambropoulou, D.A.; Evgenidou, E.; Saliverou, V.; Kosma, C.I.; Konstantinou, I.K. Degradation of venlafaxine using TiO_2/UV process: Kinetic studies, RSM optimization, identification of transformation products and toxicity evaluation. *J. Hazard. Mater.* **2017**, *323*, 513–526. [CrossRef] [PubMed]
23. Stapleton, D.R.; Konstantinou, I.K.; Mantzavinos, D.; Hela, D.; Papadaki, M. On the kinetics and mechanisms of photolytic/TiO_2-photocatalytic degradation of substituted pyridines in aqueous solutions. *Appl. Catal. B Environ.* **2010**, *95*, 100–109. [CrossRef]
24. Antonopoulou, M.; Konstantinou, I. Optimization and Modeling of the Photocatalytic Degradation of the Insect Repellent DEET in Aqueous TiO_2 Suspensions. *CLEAN—Soil Air Water* **2013**, *41*, 593–600. [CrossRef]

25. Antonopoulou, M.; Konstantinou, I. Photocatalytic treatment of metribuzin herbicide over TiO2aqueoussuspensions: Removal efficiency, identification of transformationproducts, reaction pathways and ecotoxicity evaluation. *J. Photochem. Photobiol. A Chem.* **2014**, *294*, 110–120. [CrossRef]
26. Antonopoulou, M.; Konstantinou, I. TiO_2 photocatalysis of 2-isopropyl-3-methoxy pyrazine taste and odor compound in aqueous phase: Kinetics, degradation pathways and toxicity evaluation. *Catal. Today* **2015**, *240*, 22–29. [CrossRef]
27. Stamatis, N.; Antonopoulou, M.; Hela, D.; Konstantinou, I.K. Photocatalytic degradation kinetics and mechanisms of antibacterial triclosan in aqueous TiO_2 suspensions under simulated solar irradiation. *J. Chem. Technol. Biotechnol.* **2014**, *89*, 1145–1154. [CrossRef]
28. Berberidou, C.; Kitsiou, V.; Kazala, E.; Lambropoulou, D.A.; Kouras, A.; Kosma, C.I.; Albanis, T.A.; Poulios, I. Study of the decomposition and detoxification of the herbicidebentazon by heterogeneous photocatalysis: Kinetics, intermediatesand transformation pathways. *Appl. Catal. B Environ.* **2017**, *200*, 150–163. [CrossRef]
29. Koltsakidou, A.; Antonopoulou, M.; Evgenidou, E.; Konstantinou, I.; Giannakas, A.E.; Papadaki, M.; Bikiaris, D.; Lambropoulou, D.A. Photocatalytical removal of fluorouracil using TiO_2-P25 and N/S doped TiO_2 catalysts: A kinetic and mechanistic study. *Sci. Total Environ.* **2017**, *578*, 257–267. [CrossRef]
30. Moreira, N.; Sampaio, M.; Ribeiro, A.; Silva, C.; Faria, J.; Silva, A. Metal-free g-C_3N_4 photocatalysis of organic micropollutants in urban wastewater under visible light. *Appl. Catal. B Environ.* **2019**, *248*, 184–192. [CrossRef]
31. Ding, N.; Chang, X.; Shi, N.; Yin, X.; Qi, F.; Sun, Y. Enhanced inactivation of antibiotic-resistant bacteria isolated from secondary effluents by g-C_3N_4 photocatalysis. *Environ. Sci. Pollut. Res.* **2019**, *26*, 18730–18738. [CrossRef] [PubMed]
32. Hu, J.; Zhang, P.; An, W.; Liu, L.; Liang, Y.; Cui, W. In-situ Fe-doped g-C_3N_4 heterogeneous catalyst via photocatalysis-Fenton reaction with enriched photocatalytic performance for removal of complex wastewater. *Appl. Catal. B Environ.* **2019**, *245*, 130–142. [CrossRef]
33. Hu, C.; Wang, M.-S.; Chen, C.-H.; Chen, Y.-R.; Huang, P.-H.; Tung, K.-L. Phosphorus-doped g-C_3N_4 integrated photocatalytic membrane reactor for wastewater treatment. *J. Memb. Sci.* **2019**, *580*, 1–11. [CrossRef]
34. Song, Y.; Qi, J.; Tian, J.; Gao, S.; Cui, F. Construction of Ag/g-C_3N_4 photocatalysts with visible-light photocatalytic activity for sulfamethoxazole degradation. *Chem. Eng. J.* **2018**, *341*, 547–555. [CrossRef]
35. Tripathi, A.; Narayanan, S. Skeletal tailoring of two-dimensional π-conjugated polymer (g-C_3N_4) through sodium salt for solar-light driven photocatalysis. *J. Photochem. Photobiol. A* **2019**, *373*, 1–11. [CrossRef]
36. Kumar, A.; Schuerings, C.; Kumar, S.; Kumar, A.; Krishnan, V. Perovskite-structured $CaTiO_3$ coupled with g-C_3N_4 as a heterojunction photocatalyst for organic pollutant degradation. *Beilstein. J. Nanotechnol.* **2018**, *9*, 671–685. [CrossRef]
37. Domínguez-Espíndola, R.B.; Varia, J.C.; Álvarez-Gallegos, A.; Ortiz-Hernández, M.L.; Peña-Camacho, J.L.; Silva-Martínez, S. Photoelectrocatalytic inactivation of fecal coliform bacteria in urban wastewater using nanoparticulated films of TiO_2 and TiO_2/Ag. *Environ. Technol.* **2017**, *38*, 606–614. [CrossRef]
38. Li, X.; Xiong, J.; Gao, X.; Huang, J.; Feng, Z.; Chen, Z.; Zhu, Y. Recent advances in 3D g-C_3N_4 composite photocatalysts for photocatalytic water splitting, degradation of pollutants and CO_2 reduction. *J. Alloy. Compd.* **2019**, *802*, 196–209. [CrossRef]
39. Sun, L.; Li, J.; Li, X.; Liu, C.; Wang, H.; Huo, P.; Yan, Y.S. Molecularly imprinted Ag/Ag_3VO_4/g-C_3N_4 Z-scheme photocatalysts for enhanced preferential removal of tetracycline. *J. Colloid Interface Sci.* **2019**, *552*, 271–286. [CrossRef]
40. Mohapatra, D.P.; Brar, S.K.; Daghrir, R.; Tyagi, R.D.; Picard, P.; Surampalli, R.Y.; Drogui, P. Photocatalytic degradation of carbamazepine in wastewater by using a new class of whey-stabilized nanocrystalline TiO_2 and ZnO. *Sci. Total Environ.* **2014**, *485–486*, 263–269. [CrossRef]
41. Kosma, C.I.; Nannou, C.I.; Boti, V.I.; Albanis, T.A. Psychiatrics and selected metabolites in hospital and urban wastewaters: Occurrence, removal, mass loading, seasonal influence and risk assessment. *Sci. Total Environ.* **2019**, *659*, 1473–1483. [CrossRef] [PubMed]
42. Konstas, P.-S.; Konstantinou, I.; Petrakis, D.; Albanis, T. Synthesis, Characterization of g-C_3N_4/$SrTiO_3$ Heterojunctions and Photocatalytic Activity for Organic Pollutants Degradation. *Catalysts* **2018**, *8*, 554. [CrossRef]

43. Papageorgiou, M.; Kosma, C.I.; Lambropoulou, D.A. Seasonal occurrence, removal, mass loading and environmental risk assessment of 55 pharmaceuticals and personal care products in a municipal wastewater treatment plant in Central Greece. *Sci. Total Environ.* **2016**, *543*, 547–569. [CrossRef] [PubMed]
44. Gros, M.; Rodriguez-Mozaz, S.; Barcelo, D. Rapid analysis of multiclass antibiotic residues and some of their metabolites in hospital, urban wastewater and river water by ultra-high-performance liquid chromatography coupled to quadrupole-linear ion trap tandem mass spectrometry. *J. Chromatogr. A* **2013**, *1292*, 173–188. [CrossRef] [PubMed]
45. García-Galána, M.J.; Anfruns, A.; Gonzalez-Olmos, R.; Rodríguez-Mozaz, S.; Comas, J. UV/H_2O_2 degradation of the antidepressants venlafaxine and O-desmethylvenlafaxine: Elucidation of their transformation pathwayand environmental fate. *J. Hazard. Mater.* **2016**, *311*, 70–80. [CrossRef] [PubMed]
46. Skibinski, R. Identification of photodegradation product of amisulpride by ultra-high-pressure liquid chromatography–DAD/ESI-quadrupole time-of-flight-mass spectrometry. *J. Pharm. Biomed. Anal.* **2011**, *56*, 904–910. [CrossRef] [PubMed]
47. Gros, M.; Williams, M.; Llorca, M.; Rodriguez-Mozaz, S.; Barceló, D.; Kookana, R.S. Photolysis of the antidepressants amisulpride and desipramine in wastewaters: Identification of transformation products formed and their fate. *Sci. Total Environ.* **2015**, *530–531*, 434–444. [CrossRef]
48. Jelic, A.; Michael, I.; Achilleos, A.; Hapeshi, E.; Lambropoulou, D.; Perez, S.; Petrovic, M.; Fatta-Kassinos, D.; Barcelo, D. Transformation products and reaction pathways of carbamazepineduring photocatalytic and sonophotocatalytic treatment. *J. Hazard. Mater.* **2013**, *263*, 177–186. [CrossRef]
49. Petrovic, M.; Barcelo, D. LC-MS for identifying photodegradation products of pharmaceuticals in the environment. *Trends Anal. Chem.* **2007**, *26*, 486–493. [CrossRef]
50. Daniele, G.; Fieu, M.; Joachim, S.; Bado-Nilles, A.; Beaudouin, R.; Baudoin, P.; James-Casas, A.; Andres, S.; Bonnard, M.; Bonnard, I.; et al. Determination of carbamazepine and 12 degradation products in various compartments of an outdoor aquatic mesocosm by reliable analytical methods based on liquid chromatography-tandem mass spectrometry. *Environ. Sci. Pollut. Res.* **2017**, *24*, 16893–16904. [CrossRef]
51. Ioannidou, E.; Frontistis, Z.; Antonopoulou, M.; Venieri, D.; Konstantinou, I.; Kondarides, D.I.; Mantzavinos, D. Solar photocatalytic degradation of sulfamethoxazole over tungsten—Modified TiO_2. *Chem. Eng. J.* **2017**, *318*, 143–152. [CrossRef]
52. Mirzaei, A.; Yerushalmi, L.; Chen, Z.; Haghighat, F. Photocatalytic degradation of sulfamethoxazole by hierarchical magnetic ZnO@g-C_3N_4: RSM optimization, kinetic study, reaction pathway and toxicity evaluation. *J. Hazard. Mater.* **2018**, *359*, 516–526. [CrossRef] [PubMed]
53. Konstantinou, I.K.; Sakkas, V.A.; Albanis, T.A. Photocatalytic degradation of the herbicides propanil and molinate over aqueous TiO_2 suspensions: Identification of intermediates and the reaction pathway. *Appl. Catal. B Environ.* **2001**, *34*, 227–239. [CrossRef]
54. Konstantinou, I.K.; Albanis, T.A. Photocatalytic transformation of pesticides in aqueous titanium dioxide suspensions using artificial and solar light: Intermediates and degradation pathways. *Appl. Catal. B Environ.* **2002**, *1310*, 1–17. [CrossRef]
55. Sakkas, V.A.; Konstantinou, I.K.; Albanis, T.A. Photodegradation study of the antifouling booster biocide dichlofluanid in aqueous media by gas chromatographic techniques. *J. Chromatogr. A* **2001**, *930*, 135–144. [CrossRef]
56. Czech, B.; Tyszczuk-Rotko, K. Caffeine hinders the decomposition of acetaminophen over TiO_2-SiO_2 nanocomposites containing carbon nanotubes irradiated by visible light. *J. Photochem. Photobiol. A Chem.* **2019**, *376*, 166–174. [CrossRef]
57. Choi, J.; Lee, H.; Choi, Y.; Kim, S.; Lee, S.; Lee, S.; Choic, W.; Lee, J. Heterogeneous photocatalytic treatment of pharmaceuticalmicropollutants: Effects of wastewater effluent matrix and catalyst modifications. *Appl. Catal. B Environ.* **2014**, *147*, 8–16. [CrossRef]
58. Mphela, R.K.; Msimanga, W.; Pete, K.Y.; Chiririwa, H.; Ochieng, A. Photocatalytic Degradation of Salicylic Acid and Reduction of Cr(VI) using TiO_2. In Proceedings of the 5th International Conference on Advances in Engineering and Technology (ICAET'2016), New York, NY, USA, 8–9 June 2016; p. 30.
59. Vilhunen, S.; Bosund, M.; Kaariainen, M.-L.; Cameron, D.; Sillanpaa, M. Atomic layer deposited TiO_2 films in photodegradation of aqueous salicylic acid. *Sep. Purif. Technol.* **2009**, *66*, 130–134. [CrossRef]

60. Zhao, D.; Chen, C.; Wang, Y.; Ji, H.; Ma, W.; Zang, L.; Zhao, J. Surface Modification of TiO2 by Phosphate: Effect on Photocatalytic Activity and Mechanism Implication. *J. Phys. Chem. C* **2008**, *112*, 5993–6001. [CrossRef]
61. Kosma, C.I.; Lambropoulou, D.A.; Albanis, T.A. Photochemical transformation and wastewater fate and occurrence of omeprazole: HRMS for elucidation of transformation products and target and suspect screening analysis in wastewaters. *Sci. Total Environ.* **2017**, *590–591*, 592–601. [CrossRef]